Chapter 166
Build-up Analysis of Multi-Well System in Naturally Fractured HTHP Gas Reservoirs

Hedong Sun[1(✉)], Yongping Cui[2], Xiaopei Wang[3], Jianye Zhang[3], and Wen Cao[1]

[1] Research Institute of Exploration and Development, PetroChina, Beijing, China
{sunhed, caow69}@petrochina.com.cn
[2] PetroChina Exploration and Production Company, Beijing, China
cuiyp@petrochina.com.cn
[3] Tarim Oilfield Company, PetroChina, Beijing, China
{wxpei-tlm, zhangjy-tlm}@petrochina.com.cn

Nomenclature

B	Formation-volume factor
C	WBS coefficient, m^3/Pa
C_t	Total compressibility, Pa^{-1}
h	Net-pay thickness, m
K	Permeability, m^2
K_0	Bessel function
K_1	Bessel function
m	$m = 2\int \frac{p}{\mu Z} dp$, MPa^2/mPa s
p_i	Initial pressure, Pa
q_j	Rate, m^3/s
r_w	Wellbore radius, m
S	Skin factor
z	Laplace variable
C_D	$C_D = \frac{C}{2\pi\varphi h C_t r_w^2}$
p_D	$p_{jD} = \frac{2\pi Kh(p_i - p_{wf})}{q_1 \mu B}$
q_{jD}	$q_{jD} = \frac{q_j}{q_1}$

This paper was prepared for presentation at the 2017 International Field Exploration and Development Conference in Chengdu, China, 21–22 September 2017.

Z. Qu and J. Lin (eds.), *Proceedings of the International Field Exploration and Development Conference 2017*, Springer Series in Geomechanics and Geoengineering, https://doi.org/10.1007/978-981-10-7560-5_166

r_D $r_D = \frac{r}{r_w e^{-s}}$
t_D Dimensionless time, $t_D = \frac{Kt}{\varphi \mu C_t r_w^2}$
t_p Production time, hour
t_{pD} Dimensionless production time
Δt_D Dimensionless shut in time
a $\frac{\lambda C_D}{\omega(1-\omega)}$
b $\frac{\lambda C_D}{(1-\omega)}$
D Diffusivity ratio for composite reservoir, $D = (k/\phi\mu c_t)_2/(k/\phi\mu c_t)_1$
D Non-Darcy flow coefficient
M Mobility ratio for composite reservoir, $M = (k/\mu)_2/(k/\mu)_1$
N Number of wells
r Distance from the well test wellbore, m
R_i Outer radius of inner zone annulus in radial-composite model, m
t Time, h
Δt Shut in time, h

Greek symbols
ϕ Porosity
λ Interporosity flow coefficient
μ Viscosity, cp
ω Storativity ratio

Subscripts
D Dimensionless variable
f Fracture
m Matrix
j Index
w Wellbore conditions
wf Flowing wellbore conditions
ws Shut in wellbore conditions

166.1 Introduction

Gas reservoir dynamic description technology based on single-well pressure transient analysis (PTA) technology [1] and modern decline curve analysis (DCA) technology [2] has been widely applied in gas reservoirs with small drainage area and poor interwell communication. However, for gas reservoirs with high permeability and good interwell communication (or similar to a multi-well system), pressure build-up (PBU) information is easily affected by offset wells. Pressure derivative curve can be

downwarp or upwarp in the middle or later period. Similar cases can occur in well testing for sweet spot gas wells in reservoirs with lower permeability. The diagnostic shape is usually interpreted as boundary effect by normal single-well PTA analysis. This inaccurate interpretation will mislead decision for oil and gas field development.

Superposition is usually used in pressure analysis for a multi-well system. Lin et al. [3–12] established a perfect PBU well test analysis method for a production–injection system. Marhaendrajana et al. [13] established a well test analysis method for a multi-gas well system with offset gas wells producing simultaneously, which improved the reliability of result. Liu [14] established a type curve pattern for two wells producing simultaneously. Jia [15, 16] extended the method for multiple wells in an infinite homogeneous reservoir. Deng [17] presents a method for analysing pressure build-up data in a multi-well reservoir when the testing well, and offset wells are shutting in at the same time. A phenomenon of "upwarp" shown by pressure derivative curves in the later period was observed under all the above scenarios. However, it has not been proved theoretically.

In this work, a multi-well testing model was firstly established for an infinite homogenous and double porosity reservoir. Type curves were plotted for well test with offset wells producing or shutting in simultaneously. Through a further theoretical study on the pressure derivative curve, a new well test method considering the interference from offset wells was established for multi-well PBU analysis.

166.2 Type Curves for Multi-Well System in Infinite Homogenous Reservoir

166.2.1 Well Test Model for Multi-Well System

Assume there are N wells producing under a constant pressure in an infinite homogeneous reservoir. Gravity and capillary force influence are neglected. Skin and wellbore storage (WBS) of the well under testing are considered, while those of its offset wells are neglected. Based on the effective radius model (subscript "1" refers testing well), the definite problem can be solved as follows:

$$\frac{1}{r_{\mathrm{D}}}\frac{\partial}{\partial r_{\mathrm{D}}}\left(r_{\mathrm{D}}\frac{\partial p_{1\mathrm{D}}}{\partial r_{\mathrm{D}}}\right)=\frac{1}{C_{\mathrm{D}}\mathrm{e}^{2S}}\frac{\partial p_{1\mathrm{D}}}{\partial(t_{\mathrm{D}}/C_{\mathrm{D}})} \tag{166.1}$$

$$p_{1\mathrm{D}}(r_{\mathrm{D}},0)=0 \tag{166.2}$$

$$\frac{\mathrm{d}p_{\mathrm{wD}}}{\mathrm{d}(t_{\mathrm{D}}/C_{\mathrm{D}})}-\left(r_{\mathrm{D}}\frac{\partial p_{1\mathrm{D}}}{\partial r_{\mathrm{D}}}\right)_{r_{\mathrm{D}}=1}=1 \tag{166.3}$$

$$p_{\mathrm{wD}}=p_{1\mathrm{D}}(1,t_{\mathrm{D}}/C_{\mathrm{D}}) \tag{166.4}$$

$$p_{1\mathrm{D}}(r_{\mathrm{D}}\to\infty,0)=0 \tag{166.5}$$

For other $N-1$ wells, the diffusion equation, the initial condition, and the boundary condition are similar to the well under testing. However, the inner boundary condition is described as follows:

$$-\left(r_{\mathrm{D}}\frac{\partial p_{j\mathrm{D}}}{\partial r_{\mathrm{D}}}\right)_{r_{\mathrm{D}}=1}=q_{j\mathrm{D}}\quad j=2,3\ldots,N \tag{166.6}$$

166.2.2 Solution Procedure

With Laplace transforms, the bottomhole pressure for testing well can be described as follows:

$$\bar{p}_{\mathrm{wD}}(z)=\frac{1}{z}\left[\frac{K_0(\sigma)+\sum_{j=2}^{N}q_{j\mathrm{D}}K_0\left(\sigma r_{j\mathrm{D}}\right)}{zK_0(\sigma)+\sigma K_1(\sigma)}\right],\quad \sigma=\sqrt{\frac{z}{C_{\mathrm{D}}\mathrm{e}^{2S}}} \tag{166.7}$$

With Laplace transforms, the bottomhole pressure of offset wells can be described as follows:

$$\bar{p}_{j\mathrm{D}}\left(z,r_{j\mathrm{D}}\right)=\frac{q_{j\mathrm{D}}K_0\left(\sigma r_{j\mathrm{D}}\right)}{z\sigma K_1(\sigma)},\quad \sigma=\sqrt{\frac{z}{C_{\mathrm{D}}\mathrm{e}^{2S}}},\quad j=2,3\ldots,N \tag{166.8}$$

The Euclidean space solution for the bottomhole pressure can be obtained by the Stehfest [18] numerical inversion. If the production is zero for offset wells, Eq. 166.7 can be regarded as an effective radius bottomhole pressure (BHP) solution for the constant production well in an infinite homogeneous reservoir. In the case of a gas reservoir, dimensionless pressure should be calculated based on a normalized pseudopressure. Correspondingly, a dimensionless time should be calculated based on a normalized time. The form of the solution is similar to that given by Eqs. 166.7 and 166.8.

166.2.3 Type Curve for Pressure Drawdown for Multi-Well Producing Simultaneously

166.2.3.1 Different Production and Different Well Spacing for Offset Wells

According to Eq. 166.7, BHP influence to the testing well resulting from offset wells is mainly determined by the offset production and the well spacing. Figure 166.1 shows the pressure drawdown (PDD) curve with four wells producing simultaneously in an infinite homogeneous reservoir. Case (a): the dimensionless productions for the three offset wells are 1.0, 3.0, and 5.0, respectively. The related dimensionless well spacings are 10^3, 10^4, and 10^5. Case (b): the dimensionless productions for the offset wells are

1.0, 3.0, and 5.0, while the well spacings are 10^5, 10^4, and 10^3. Pressure derivative curves in both cases show four horizontal lines (IARF). The closer the offset wells are near to the testing well, the earlier the effect occurs on the derivative curves.

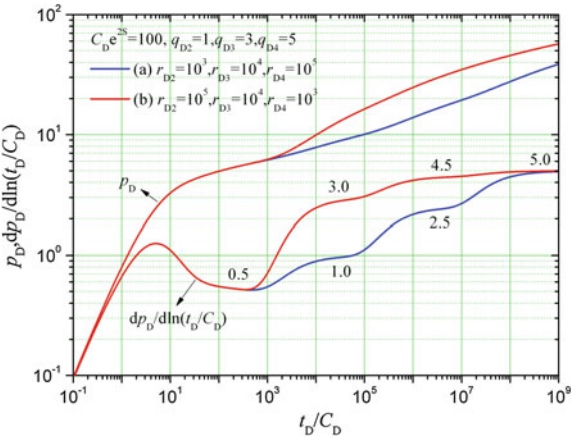

Fig. 166.1. PDD-type curve for multi-well system in infinite homogeneous reservoir. Remark—different production and different well spacing (four wells)

As shown in Case (a), for the period preceding the first IARF (0.5 line), the derivative curve is influenced by the testing well itself. For the second IARF (1.0 line), it is influenced by the testing well and the closest offset well. For the third IARF (2.5 line), it is influenced by the testing well and the top two of the closest offset wells. For the fourth IARF (5.0 line), it is influenced by the testing well and all the three offset wells. The ratios of the second, the third, and the fourth radial flow horizontal elevation to the first radial flow horizontal elevation are algebraic sum of normalized productions of the testing and offset wells, i.e., $\left(1+\sum_{j=2}^{X} q_{j\mathrm{D}}\right)$, where x is the number of offset wells affecting the testing well. For example, in Case (a), the ratio of the fourth radial flow horizontal elevation to the first radial horizontal elevation can be calculated with 5.0/0.5, i.e., 10.0. This equals to the algebraic sum of dimensionless productions, that is, 1.0 + 1.0 + 3.0 + 5.0 = 10.0. Case (b) can be explained in a similar manner.

166.2.3.2 Same Production and Different Well Spacing for Offset Wells

If the offset wells with different well spacings to the testing well can produce with the same production, four radial follows horizontal lines will also occur, as shown in Fig. 166.2. The pressure derivative curve characteristic and its explanation are the same as discussed in Fig. 166.1.

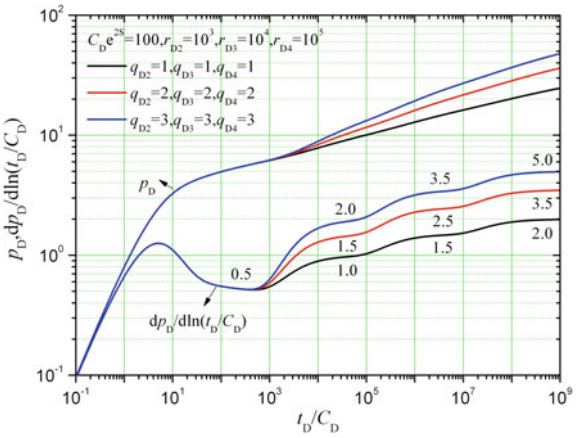

Fig. 166.2. PDD-type curve for multi-well system in infinite homogeneous reservoir. Remark—same production and different well spacing (four wells)

166.2.3.3 Similar Well Spacing with Offset Wells

If there is a similar well spacing between the testing well and each of the offset wells, only two radial flow horizontal lines will occur, as shown in Fig. 166.3. The first radial flow horizontal line reflects characteristics of the testing well (0.5 line). The second radial flow horizontal line reflects the production characteristic of the whole system (2.0, 4.0, and 5.0 line).

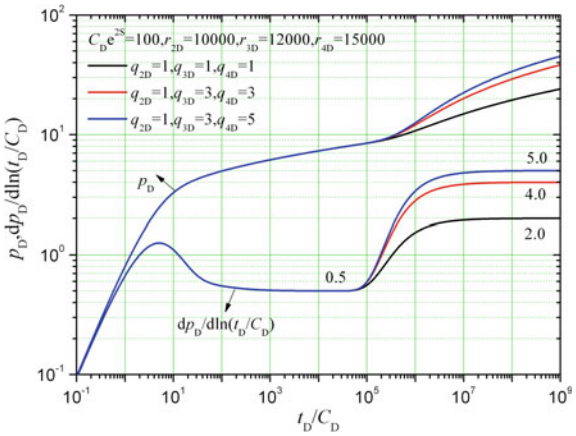

Fig. 166.3. PDD-type curve for well producing simultaneously in infinite homogeneous reservoir. Remark—same well spacing for offset wells (four wells)

166.2.3.4 Type Curve for PDD in Multi-Wells Producing Simultaneously

With variety σ small enough, Bessel [19] function can show a nature given as follows:

$$K_0(\sigma) = -\left(\ln\frac{\sigma}{2} + \gamma\right) \tag{166.9}$$

$$K_1(\sigma) = \frac{1}{\sigma} \tag{166.10}$$

Substituting Eqs. 166.9 and 166.10 into Eq. 166.7 and performing Laplace inversion transform, we have

$$p_{\mathrm{wD}} = \frac{1}{2}\left(1 + \sum_{j=2}^{N} q_{j\mathrm{D}}\right)\left[\ln\left(\frac{t_{\mathrm{D}}}{C_{\mathrm{D}}}\right) + \gamma + \ln C_{\mathrm{D}}\mathrm{e}^{2S}\right] - \sum_{j=2}^{N} q_{j\mathrm{D}}\ln r_{\mathrm{jD}} \tag{166.11}$$

Calculating the derivative with logarithmic time for Eq. 166.11, we have

$$\frac{\mathrm{d}p_{\mathrm{wD}}}{\mathrm{d}\ln\left(\frac{t_{\mathrm{D}}}{C_{\mathrm{D}}}\right)} = \frac{1}{2}\left(1 + \sum_{j=2}^{N} q_{j\mathrm{D}}\right) \tag{166.12}$$

As seen, the ratios of radial horizontal line elevations for PDD derivative curves in multi-well producing simultaneously to the single-well radial flow line elevation are the algebraic sum of normalized productions for the testing well and all connected offset wells, i.e., $\left(1 + \sum_{j=2}^{N} q_{j\mathrm{D}}\right)$. Therefore, the stepwise increase of the pressure derivative may be due to the characteristic of an impermeable boundary or a radial composite reservoir with low-mobility outer zone while it may result from the interference between wells.

166.2.4 PBU-Type Curve Character and PBU Analysis for Multi-Well Shut in Simultaneously

166.2.4.1 PBU-Type Curve Character for Multi-Well Shut in Simultaneously

PBU curves for the case that the testing well and the offset wells are shut in at the same time are shown in Fig. 166.4. When $t_{\mathrm{pD}} \gg \Delta t_{\mathrm{D}}$, there is an overlap between the PDD curve and the PBU curve. When a semilog condition is assumed, the derivative of the normalized PBU pressure $p_{\mathrm{BUD}}\left(\frac{\Delta t_{\mathrm{D}}}{C_{\mathrm{D}}}\right)$ about $\frac{\Delta t_{\mathrm{D}}}{C_{\mathrm{D}}}$ is

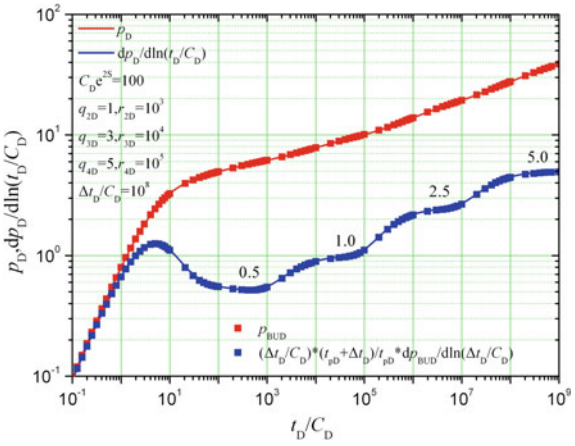

Fig. 166.4. Type curve comparison for PDD and PBU for multi-wells in infinite homogeneous reservoir Remark: four wells, PDD——producing simultaneously for multi-wells; PBU——shutin simultaneously for multi-wells

$$\frac{dp_{BUD}\left(\frac{\Delta t_D}{C_D}\right)}{d\left(\frac{\Delta t_D}{C_D}\right)}\left(\frac{\Delta t_D}{C_D}\right)\left(\frac{t_{pD}+\Delta t_D}{t_{pD}}\right)=\frac{1}{2}\left(1+\sum_{j=2}^{N}q_{jD}\right) \tag{166.13}$$

The PBU derivative curve will be "upwarp" in both of the middle and the later periods for multi-well shut in simultaneously.

The PBU pressure derivative for the testing well can be solved as follows:

$$\frac{dp_{BUD}\left(\frac{\Delta t_D}{C_D}\right)}{d\left(\frac{\Delta t_D}{C_D}\right)}\left(\frac{\Delta t_D}{C_D}\right)\left(\frac{t_{pD}+\Delta t_D}{t_{pD}}\right)=\frac{1}{2}\left[1-\sum_{j=2}^{N}q_{jD}\times\left(\frac{\Delta t_D}{t_{pD}}\right)\right] \tag{166.14}$$

Therefore, when there is consistent interference from the offset wells under producing to the testing well pressure, PBU derivative curve of the testing well will be "downwarp" in both of the middle and the later periods, as shown in Fig. 166.5.

Downwarp velocity is decided by the algebraic sum of normalized productions of the offset wells which influence the testing well, i.e., $\sum_{j=2}^{X} q_{jD}$,and the ratio of the shutin time to the production time before shutin, i.e., $\frac{\Delta t_D}{t_{pD}}$.

166.2.4.2 Analysis Procedure for PBU for Multi-Wells Shutin Simultaneously

The procedure for analysing a multi-well system is similar to that of a single-well system [20]. The key steps are as follows:

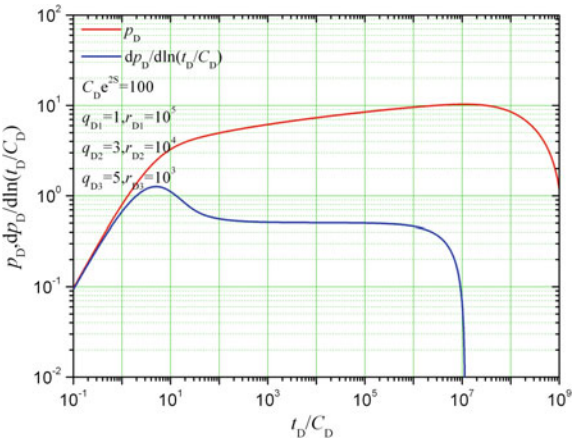

Fig. 166.5. PBU-type curve for offset wells producing in multi-wells system in infinite homogeneous reservoir

(1) Calculate the differential pressure within all the testing points $\Delta p_{ws}(\Delta t) = p_{ws}(\Delta t) - p_{wf}(t_p)$ and the related pressure derivative $\frac{d\Delta p_{ws}}{d\Delta t} \times \Delta t \times \frac{t_p + \Delta t}{t_p}$. In the case of gas wells, analysis can be performed with the pseudopressure.
(2) Fit testing points with the PDD-type curve. According to the fitted valves of abscissa axis, ordinate axis and the curve, parameters including *Kh, S,* and *C* can be calculated, respectively.
(3) Calculate ratios of each radial flow horizontal line elevation to the first radial flow horizontal line elevation, i.e., $\left(1 + \sum_{j=2}^{N} q_{jD}\right)$. On that basis, estimate the interference sequence and the corresponding number of offset wells.

According to the log–log analysis, further numerical well test analysis and history matching can be performed, which can deliver a further improved interpretation on the well test result.

166.3 Type Curves for Multi-Well System in Infinite Double Porosity Reservoir

166.3.1 Well Test Model and Solution Procedure

Assume there are *N* wells producing at a constant production in an infinite double porosity reservoir, where the gravity and capillary force can be neglected. Skin and WBS of the testing well are considered, while those of offset wells are neglected. Based on the effective well radius model, a definite solution for the testing well (subscript "1" refers to testing well) can be described as follows:

$$\frac{1}{r_{\mathrm{D}}}\frac{\partial}{\partial r_{\mathrm{D}}}\left(r_{\mathrm{D}}\frac{\partial p_{\mathrm{fD}}}{\partial r_{\mathrm{D}}}\right)=\frac{1-\omega}{C_{\mathrm{D}}\mathrm{e}^{2S}}\frac{\partial p_{\mathrm{mD}}}{\partial(t_{\mathrm{D}}/C_{\mathrm{D}})}+\frac{\omega}{C_{\mathrm{D}}\mathrm{e}^{2S}}\frac{\partial p_{\mathrm{fD}}}{\partial(t_{\mathrm{D}}/C_{\mathrm{D}})} \tag{166.15}$$

$$\frac{1-\omega}{C_{\mathrm{D}}\mathrm{e}^{2S}}\frac{\partial p_{\mathrm{mD}}}{\partial(t_{\mathrm{D}}/C_{\mathrm{D}})}=\frac{\lambda}{\mathrm{e}^{2S}}(p_{\mathrm{fD}}-p_{\mathrm{mD}}) \tag{166.16}$$

$$p_{\mathrm{fD}}(r_{\mathrm{D}},0)=p_{\mathrm{mD}}(r_{\mathrm{D}},0)=0 \tag{166.17}$$

$$\frac{\mathrm{d}p_{\mathrm{wfD}}}{\mathrm{d}(t_{\mathrm{D}}/C_{\mathrm{D}})}-\left(r_{\mathrm{D}}\frac{\partial p_{\mathrm{fD}}}{\partial r_{\mathrm{D}}}\right)_{r_{\mathrm{D}}=1}=1 \tag{166.18}$$

$$p_{\mathrm{wfD}}=p_{\mathrm{fD}}(1,t_{\mathrm{D}}/C_{\mathrm{D}}) \tag{166.19}$$

$$p_{\mathrm{fD}}(r_{\mathrm{D}}\to\infty,0)=0 \tag{166.20}$$

The diffusion equation, initial conditions, and exterior conditions of the other $N-1$ offset wells are similar to those of the testing well in the definite solution. Meanwhile, the inner boundary is described as

$$-\left(r_{\mathrm{D}}\frac{\partial p_{j\mathrm{fD}}}{\partial r_{\mathrm{D}}}\right)_{r_{\mathrm{D}}=1}=q_{j\mathrm{D}}\quad j=2,3\ldots,N \tag{166.21}$$

With Laplace transform, accurate BHP of the testing well can be obtained as

$$\begin{aligned}\bar{p}_{\mathrm{wD}}(z)&=\frac{1}{z}\left[\frac{K_0(\sigma)+\sum_{j=2}^{N}q_{j\mathrm{D}}K_0\left(\sigma r_{j\mathrm{D}}\right)}{zK_0(\sigma)+\sigma K_1(\sigma)}\right],\quad \sigma=\sqrt{\frac{z}{C_{\mathrm{D}}\mathrm{e}^{2S}f(z)}},\\ f(z)&=\frac{\lambda C_{\mathrm{D}}+\omega(1-\omega)z}{\lambda C_{\mathrm{D}}+(1-\omega)z}\end{aligned} \tag{166.22}$$

166.3.2 Approximate Solution for Long-Term Asymptotic Solutions

166.3.2.1 Approximate Solution for PDD in a Multi-Well System

According to Eq. 166.22, the approximate solution for PDD with multi-wells producing simultaneously can be given by

$$p_{\mathrm{wfD}}=\frac{1}{2}\left(1+\sum_{j=2}^{N}q_{j\mathrm{D}}\right)\left[\begin{array}{l}\ln\left(\frac{t_{\mathrm{D}}}{C_{\mathrm{D}}}\right)+Ei\left(-a\frac{t_{\mathrm{D}}}{C_{\mathrm{D}}}\right)\\ -Ei\left(-b\frac{t_{\mathrm{D}}}{C_{\mathrm{D}}}\right)+\ln C_{\mathrm{D}}\mathrm{e}^{2S}\\ +0.80908-2\ln r_{j\mathrm{D}}\end{array}\right] \tag{166.23}$$

The pressure derivative is

$$\frac{\mathrm{d}p_{\mathrm{wfD}}}{\mathrm{d}\ln\left(\frac{t_{\mathrm{D}}}{C_{\mathrm{D}}}\right)}=\frac{1}{2}\left(1+\sum_{j=2}^{N}q_{j\mathrm{D}}\right)\left[\begin{array}{l}1-\exp\left(-a\frac{t_{\mathrm{D}}}{C_{\mathrm{D}}}\right)\\+\exp\left(-b\frac{t_{\mathrm{D}}}{C_{\mathrm{D}}}\right)\end{array}\right] \tag{166.24}$$

166.3.2.2 Approximate Solution for PBU with Offset Wells Shut in or Producing Simultaneously

Similar to the homogenous reservoir, PBU pressure can be described as follows when testing well and offset wells are shut in simultaneously:

$$p_{\mathrm{BUD}}\left(\frac{\Delta t_{\mathrm{D}}}{C_{\mathrm{D}}}\right)=p_{\mathrm{D}}\left(\frac{t_{\mathrm{pD}}}{C_{\mathrm{D}}}\right)-p_{\mathrm{D}}\left(\frac{t_{\mathrm{pD}}+\Delta t_{\mathrm{D}}}{C_{\mathrm{D}}}\right)+p_{\mathrm{D}}\left(\frac{\Delta t_{\mathrm{D}}}{C_{\mathrm{D}}}\right) \tag{166.25}$$

The pressure derivative is

$$\frac{\mathrm{d}p_{\mathrm{BUD}}\left(\frac{\Delta t_{\mathrm{D}}}{C_{\mathrm{D}}}\right)}{\mathrm{d}\left(\frac{\Delta t_{\mathrm{D}}}{C_{\mathrm{D}}}\right)}\left(\frac{\Delta t_{\mathrm{D}}}{C_{\mathrm{D}}}\right)\left(\frac{t_{\mathrm{pD}}+\Delta t_{\mathrm{D}}}{t_{\mathrm{pD}}}\right)=\frac{1}{2}\left(1+\sum_{j=2}^{N}q_{j\mathrm{D}}\right)\left[\begin{array}{l}1-\exp\left(-a\frac{t_{\mathrm{D}}}{C_{\mathrm{D}}}\right)\\+\exp\left(-b\frac{t_{\mathrm{D}}}{C_{\mathrm{D}}}\right)\end{array}\right] \tag{166.26}$$

The pressure derivative with the testing well shut in and offset wells producing is given by

$$\begin{array}{l}\frac{1}{2}\left(1-\sum_{j=2}^{N}q_{j\mathrm{D}}\frac{\Delta t_{\mathrm{D}}}{t_{\mathrm{pD}}}\right)+\frac{1}{2}\left(1+\sum_{j=2}^{N}q_{j\mathrm{D}}\right)\left(\frac{\Delta t_{\mathrm{D}}}{t_{\mathrm{pD}}}\right)\\\left[\begin{array}{l}\exp\left(-a\frac{\Delta t_{\mathrm{D}}+t_{\mathrm{pD}}}{C_{\mathrm{D}}}\right)\\-\exp\left(-b\frac{\Delta t_{\mathrm{D}}+t_{\mathrm{pD}}}{C_{\mathrm{D}}}\right)\end{array}\right]+\frac{1}{2}\left(\frac{\Delta t_{\mathrm{D}}+t_{\mathrm{pD}}}{t_{\mathrm{pD}}}\right)\\\left[exp\left(-b\frac{\Delta t_{\mathrm{D}}}{C_{\mathrm{D}}}\right)-exp\left(-a\frac{\Delta t_{\mathrm{D}}}{C_{\mathrm{D}}}\right)\right]\end{array}$$

166.3.3 PDD-Type Curve Character for Multi-Wells Producing Simultaneously

Same as an infinite homogeneous reservoir, when multi-wells producing simultaneously in a double porosity reservoir, the ratios of the PDD radial flow horizontal line elevations to the single-well radial flow horizontal line elevation are the algebraic sums of dimensionless productions for the testing well and all the connected offset wells. The diagnostics are shown in Fig. 166.6. For the case of PBU, the result is similar and thus not discussed.

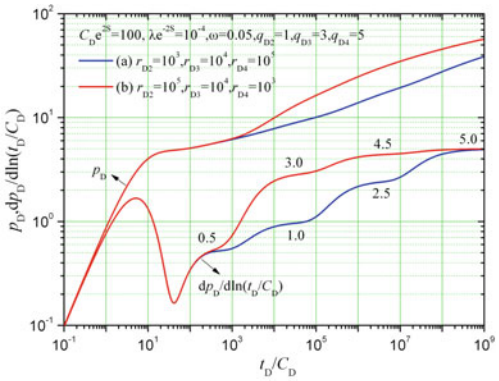

(A) Different production and different wells spacing for offset wells

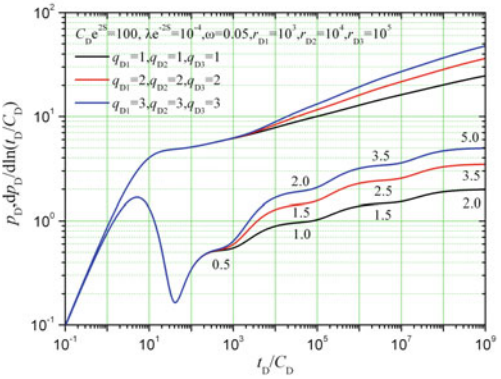

(B) Same production and different well spacing for offset wells (4 wells)

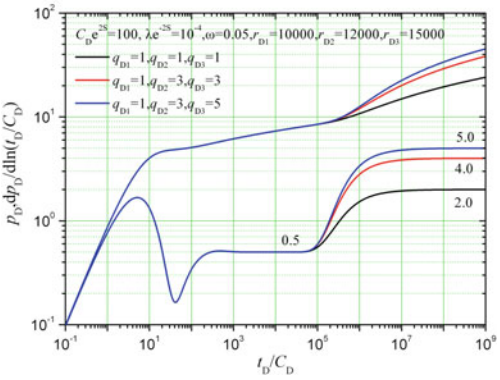

(C) Similar well spacing for offset wells (4 wells)

Fig. 166.6. PDD-type curve for multi-well system in infinite double porosity reservoir

166.4 Example

166.4.1 General Introduction for Gas Reservoir

A gas reservoir is located in northwest of China. It lies on the northwest of Kuche structure. There are little changes for the lithology and property. Porosity range is 5.5–8.0%. Matrix permeability is mainly in range of 0.01–1.0 mD. The fracture with high angle is developed. Original reservoir pressure is 89.09 MPa. Reservoir temperature is 128 °C. Gas relative density is 0.58. There are six developed wells currently as shown in Fig. 166.7.

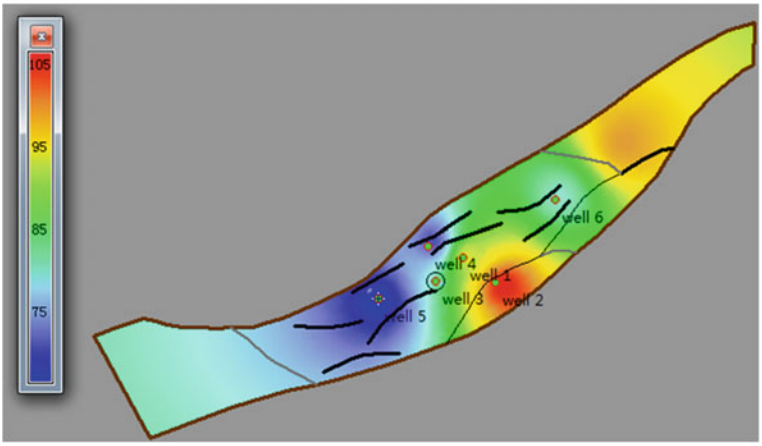

Fig. 166.7. Well location and effective net-pay map for gas reservoir

166.4.2 Production Status

There are six producers put into production in the gas reservoir. Average gas rate is about 170 × 10^4 m^3/d, cumulative gas production is 15 × 10^8 m^3, and gas production for a single well 15–45 × 10^4 m^3/d. The production performance is shown in Fig. 166.8.

During production, Well 2 was sanding and there were big changes on flowing pressure. The fracture of Well 3 was non-development, lower production, and lower flowing pressure. Field was shut in in May 2016. Except Well 3, WHP of all the other wells were build-up to a comparable value, as shown in Fig. 166.9. Flowing pressures were decreasing for wells put into production later, as given in Table 166.1. Therefore, there is a possibility for achieving connectivity within the whole gas reservoir (Fig. 166.10).

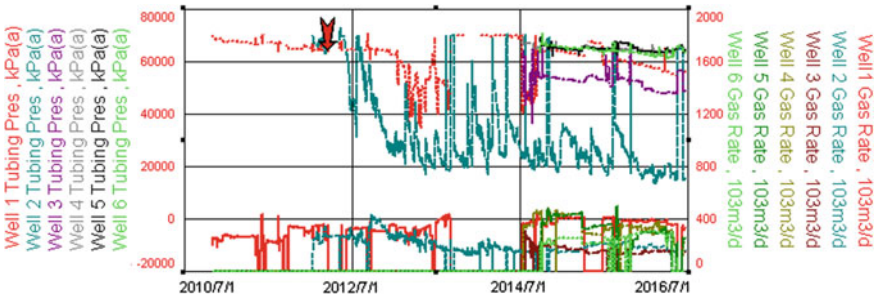

Fig. 166.8. Production performance for gas reservoir

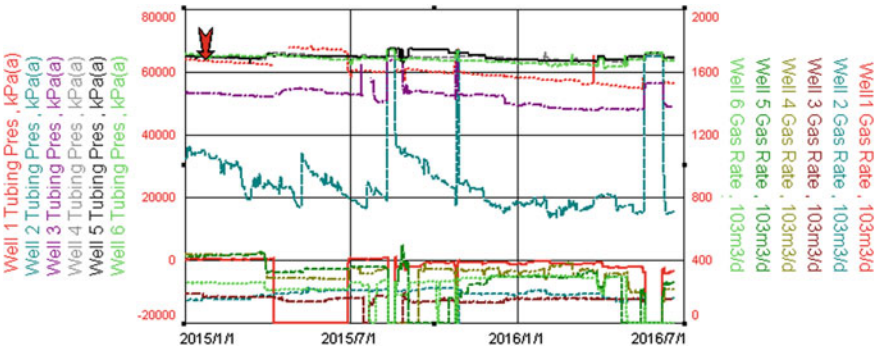

Fig. 166.9. Production curves for a gas reservoir from 2015 to May 2016

Table 166.1. Production information in a gas reservoir

Well name	Online date	Original reservoir pressure	Effective thickness (m)	Porosity (%)	Gas production (10^4 m^3/d)
Well 3	2014-7-16	79.74	87	5.6	16.5
Well 6	2014-9-29	86.06	79	6.2	25.3
Well 5	2014-9-27	84.72	65	7.1	33.0
Well 1	2010-10-30	89.09	82	6.8	33.4
Well 4	2014-7-17	85.83	69	6.9	35.3
Well 2	2012-1-11	86.74	105	7.9	20.7

166.4.3 Test Introduction

Well 5 was shut in in Aug 2015 for PBU after producing 320 days. The well was shut in for the first PBU test. The other five wells were shut in at the same time. The modified isochronal test was performed, during which the Well 1, 2, 6 were producing. At last, an extend PBU test was performed, during which Well 3 and Well 4 were back online one after another. Performance is shown in Fig. 166.10.

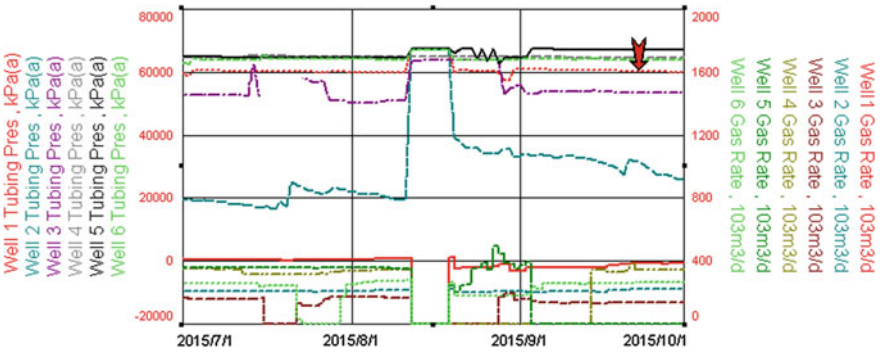

Fig. 166.10. Production curves for a gas reservoir from Jul 2015 to Oct 2016

166.4.4 Test Analysis

The log–log derivative curve is shown in Fig. 166.11. Similar to Example 1, there is an obviously difference between curve shapes of the first PBU and the last PBU curve. Directions of the curve shapes are opposite. Derivative curves for the four PBUs were upwarp during the modified isochronal test.

Although this gas reservoir is with developed fracture, interpretation is shown in Fig. 166.12 based on the double porosity model. One set of parameters could not well fit two PBU curves. In addition, it is hard to explain the difference in curve shapes of two PBUs. Considering the production dynamic, a multi-well model is selected to perform interpretation.

Considering the production dynamic, there is possible interference between producers in the gas reservoir. The ratio of average field production to the testing well production is $(16.5 + 25.3 + 33 + 33.4 + 35.3 + 20.7)/33 = 5.0$. Meanwhile, the horizontal line elevation for the first PBU derivative curve is 3.85×10^7, and the second horizontal line elevation is 20×10^7, of which the ratio is nearly 5.0. Therefore, the multi-well model in a homogeneous reservoir can be selected for interpretation, as shown in Fig. 166.13. Historical fitting for the production data is shown in Fig. 166.14. When the well was online, the original reservoir pressure had dropped from 89 to 85 MPa, while the current reservoir pressure is 81.6 MPa.

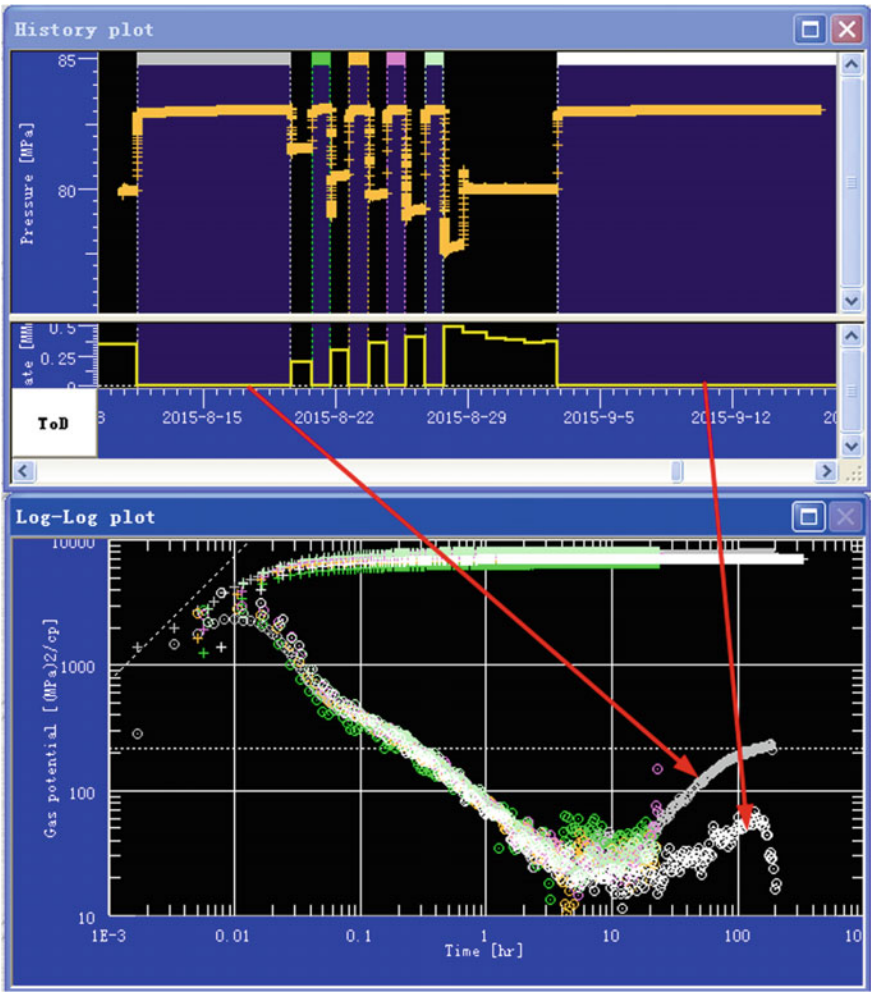

Fig. 166.11. Log–log curve for five wells testing in a gas reservoir

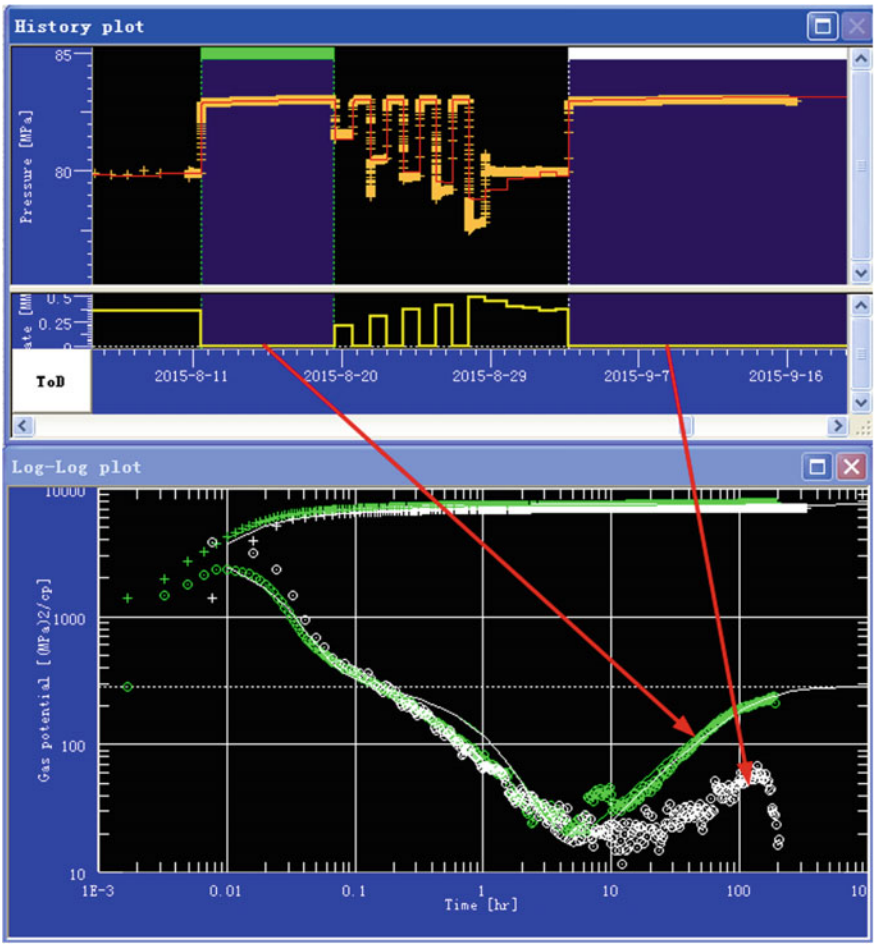

Fig. 166.12. Fitting curves for PTA analysis for five wells testing with double porosity model

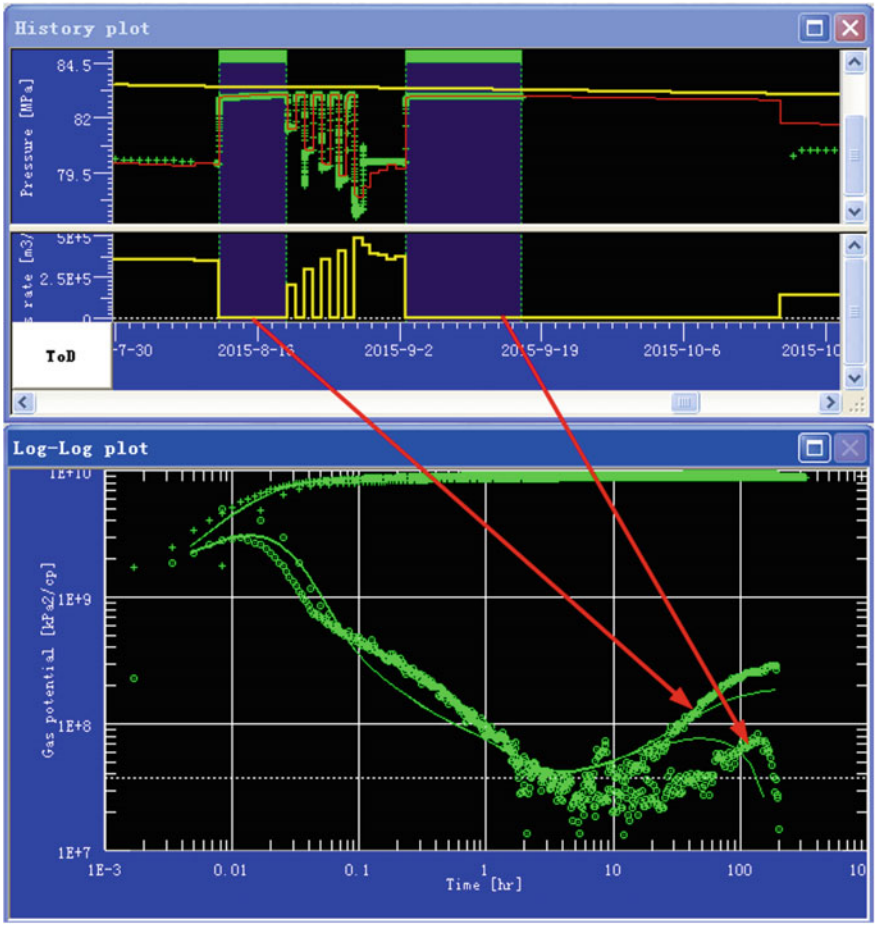

Fig. 166.13. Log–log curves for PTA analysis for five wells testing with multiple wells model

Fig. 166.14. History match curve for PTA analysis for five wells testing with multiple wells model

166.5 Conclusions

(1) Many stages can occur in the PBU derivative curve. The model of reservoir can be ① a radial composite reservoir with low-mobility outer zone;② one or multiple impermeable boundaries;③ with edge water drive for a gas well;④ influence between wells.

(2) There is an upwarp stage for a derivative curve in PBU or PDD for multi-well producing or shut in simultaneously. The ratio of each horizontal elevation to the first horizontal elevation is the algebraic sum of normalized productions for the testing and offset wells.

(3) In a multi-well system, the derivative curve will be downwarp in the PBU later period with offset wells producing simultaneously. Downwarp velocity is determined by the algebraic sum of normalized productions for effective offset wells and ratio of shut in time to the producing time before shut in.

(4) For a new proven reservoir, the reservoir boundary and the interference from offset wells can be recognized by two PBU testing. The first PBU is performed with offset wells producing. The second PBU is performed with offset wells shut in.

(5) By combining the techniques of multi-well test and multi-well modern DCA, an accurate reservoir description can be achieved for a gas reservoir with good connectivity. The analysis can provide technical support for development plan design and optimization.

References

1. Spivey JP, Lee WJ (2013) Applied well test interpretation. Society of Petroleum Engineers, Richardson, pp 1–30
2. Sun H (2015) Advanced production decline analysis and application. Gulf Professional Publishing, Oxford, pp 263–290
3. Lin J, Liu W, Chen Q (1993) Pressure buildup analysis for a well in a pressure-maintained system. Well Test 2(4):51–58
4. Lin J, Liu W, Chen Q (1996) Application of the well test analysis theory to a multiwell water flooding system. Pet Explor Dev 23(3):58–63
5. Onur M, Serra KV, Reynolds AC (1991) Analysis of pressure buildup data from a well in a multiwell system. SPE Formation Eval 6(1):101–110
6. Dong J, Zhai Y, Yang J, Zhao C (1999) Determination of injection production ratio size by type curve analysis. In: Paper SPE 57320 presented at the SPE Asia Pacific improved oil recovery conference, Kuala Lumpur, Malaysia, 25–26 Oct 1999. http://dx.doi.org/10.2118/57320-MS
7. Lin J, Yang H (2005) Pressure buildup analysis for a well in a closed, bounded multiwell reservoir. Chin J Chem Eng 13(4):441–450
8. Lin J, Yang H (2005) Analysis of two phase flow pressure buildup data from well in an infinite multiwell reservoir. J Hydrodynam Series B 17(4):489–497
9. Lin J, Yang H (2007) Analysis of well test data in a multiwell reservoir with water injection. In: Paper SPE 110349 presented at SPE annual technical conference and exhibition, Anaheim, California, USA, 11–14 Nov 2007. http://dx.doi.org/10.2118/110349-MS
10. Li X, Luo J (2009) Application of well test analysis model influenced by neighbouring wells. Well Test 18(2):5–7,11
11. Liu Y, Chen H, Zhang D, Zhou R, Liu Y (2002) Numerical well test analysis for oil wells in condition of adjacent wells influences. Well Test 11(5):4–7
12. Zhang L, Xiang Z, Li Y, Li X, Liu Q (2006) The interwell interference effect on numerical well test curve of oil-water phase. J Hydrodynam Series A 21(6):805–810
13. Marhaendrajana T, Kaczorowski NJ, Blasingame TA (1999) Analysis and interpretation of well test performance at Arun field, Indonesia. In: Paper SPE 56487 presented at the SPE annual technical conference and exhibition, Houston, TX, USA, 3–7 Oct 1999. http://dx.doi.org/10.2118/56487-MS
14. Qiguo L, Yanli C, Liehui Z, Wei W (2006) Study for disturbing test model with the well opening and its interpreting method. Well Testing 15(1):10–12
15. Zeng T, Jia Y, Wang H, Tang D, Wu Z (2006) Well testing model for finite multiwell system and type curve analysis. Xinjiang Pet Geol 27(1):86–88
16. Liu Y, Jia Y, Kang Y, Huo J (2008) Finite multiwell testing model for heavy oil thermal recovery under consideration heat loss. Drill Prod Technol 31(1):79–81
17. Deng Q, Nie R, Jia Y, Wang X, Chen Y, Xiong Y (2015) A new method of pressure buildup analysis for a well in a multiwell reservoir. In: Paper SPE 175866 presented at SPE North Africa technical conference and exhibition, Cairo, Egypt, 14–16 Sept 2015. http://dx.doi.org/10.2118/175866-MS
18. Stehfest H (1970) Algorithm 368: numerical inversion of Laplace transforms. Commun ACM 13(1):47–49
19. Abramowitz M, Stegun IA (1966) Handbook of mathematical functions. Dover Publications, New York, pp 374–375
20. Bourdet D, Whittle TM, Douglas AA, Pirard YM (1983) A new set of type curves simplifies well test analysis. World Oil 196(6):95–106